

Multimodel emission metrics for regional emissions of short lived climate forcers

Regional emission metrics for short lived climate forcers from multiple models

Authors: B. Aamaas¹, T. K. Berntsen^{1,2}, J. S. Fuglestad¹, K. P. Shine³, N. Bellouin³

¹ Center for International Climate and Environmental Research – Oslo (CICERO), PB 1129 Blindern, 0318 Oslo, Norway

² Department of Geosciences, University of Oslo, Norway

³ Department of Meteorology, University of Reading, United Kingdom

Correspondence to: B. Aamaas (borgar.aamaas@cicero.oslo.no)

Abstract

For short lived climate forcers (SLCFs), the impact of emissions depends on where and when the emissions take place. Comprehensive new calculations of various emission metrics for SLCFs are presented based on radiative forcing (RF) values calculated in four different (chemistry-transport or coupled-chemistry climate) models. We distinguish between emissions during summer (May-October) and winter ~~season~~ (November-April) for emissions ~~from-in~~ Europe, East Asia, as well as ~~from~~ the global shipping sector and global emissions. The species included in this study are aerosols and aerosols precursors (BC, OC, SO₂, NH₃), and ozone precursors (NO_x, CO, VOC), which also influence aerosols, to a lesser degree. Emission metrics for global climate responses of these emissions, as well as for CH₄, have been calculated ~~relative to CO₂~~ using Global Warming Potential (GWP) and Global Temperature change Potential (GTP), based on dedicated RF simulations by four global models. The emission metrics include indirect cloud effects of aerosols and the semi-direct forcing for BC. In addition to the standard emission metrics for pulse and sustained emissions, we have also calculated a new emission metric designed for an emission profile consisting of a ramping-up period of 15 years followed by sustained emissions, which is more appropriate for a gradual implementation of mitigation policies.

For the aerosols, the emission metric values are larger in magnitude for emissions in Europe than East Asia and for summer than winter. A variation is also observed for the ozone precursors, with largest values for emissions in East Asia and winter for CO and in Europe and summer for VOC. In general, the variations between the emission metrics derived from different models are larger than the variations between regions and seasons, but the regional and seasonal variations for the best estimate also hold for most of the models individually. Further, the estimated climate impact of an illustrative mitigation policy package is robust even when accounting for the fact that the magnitude of emission metrics for different species in a given model are correlated~~correlations~~. For the ramping

up emission metrics, the values are generally larger than for pulse or sustained emissions, which holds for all SLCFs. For ~~a potential~~ SLCFs mitigation policies, the dependency of metric values on the region and season of emission should be considered.

1. Introduction

Climate is impacted by various emitted gases and particles with a range of radiative efficiencies, lifetimes, and climate efficacies (e.g., Myhre et al., 2013). Emissions of CO₂, N₂O, and some of the other gases included in the Kyoto Protocol are defined as long-lived greenhouse gases (LLGHGs). In addition, emissions of black carbon (BC), organic carbon (OC), SO₂, NH₃, NO_x, CO, and volatile organic compound (VOC) cause changes in atmospheric levels of short lived climate forcers (SLCFs), such as ozone and aerosols (BC, OC, sulphate and nitrate). As CH₄ has an atmospheric perturbation lifetime of about 10 years, this gas is generally as well-mixed. CH₄ is a well-mixed gas as the LLGHGs, but is often categorized together with the SLCFs since its lifetime is shorter than a realistic time-scale for stabilizing anthropogenic influence on climate. There has recently been increased interest by policy makers to mitigate these SLCFs, for instance as advocated by the Climate and Clean Air Coalition (CCAC) motivated by co-benefits to climate and air quality (e.g., Schmale et al., 2014). Smith and Mizrahi (2013) find that the climate benefits for the next few decades of reducing SLCFs today are comparable to a climate policy on LLGHGs ~~(Smith and Mizrahi, 2013)~~. However, Myhre et al. (2011) point out that reducing emissions of SLCFs today might potentially result in a delay in CO₂ mitigation, which may give unwanted long-term consequences (Pierrehumbert, 2014). Studies show that climate change in the long term is mainly governed by CO₂ emissions; however, mitigation of SLCFs may temporarily decrease the rate of warming (Shoemaker et al., 2013; Bowerman et al., 2013). Rogelj et al. (2014) argue that quantifying the climate impact of actual mitigation ~~onng~~ policies targeted on SLCFs is difficult, as the sources are common for a range of SLCFs and LLGHGs; thus, these linkages should be considered. Recently Allen et al. (2016) showed that the Global Warming Potential with a time horizon of 100 years (GWP(100)) effectively measures the relative impact of both cumulative species and SLCFs on realized warming 20-40 years after the time of emission. They also showed that GWP(100) can be used to approximately equate a one-off pulse emission of a cumulative pollutant and an indefinitely sustained change in the rate of emission of an SLCFs, which introduces a new application when SLCFs, CO₂, and other LLGHGs are compared.

The impact of emissions of different SLCFs may be measured with the use of emission metrics which quantify an idealized climate impact per unit mass of emissions of a given species. Various applications exist (Fuglestad et al., 2003; Tanaka et al., 2010; Aamaas et al., 2013), the main ones are to 1) provide an “exchange rate” between different emitted species used in mitigation policies, 2) compare different activities and technologies that emit a range of species over time such as in Life Cycle Assessment (LCA), and 3) compare in a simplified manner the climate responses of various emissions to gain and communicate scientific understanding. The most common emission metrics are time integrated radiative forcing (Absolute Global Warming Potential, AGWP) (IPCC, 1990) and temperature perturbation (Absolute Global Temperature change Potential, AGTP) (Shine et al., 2005; Shine et al., 2007), which, when normalized to CO₂, become GWP and GTP, respectively. Physically based metrics evaluate the idealized climate impact (integrated global mean RF for GWP or global mean temperature change for the GTP) over a certain time period (for the GWP) or at a given time after the emissions (for the GTP). This time period is called the time horizon and this choice is inevitably influenced by value judgments. Here we present metric values for a range of time horizons. Among the value choices are for instance looking at either temperature or forcing and what time

horizon to pick (Fuglestad et al., 2003; Tol et al., 2012; Myhre et al., 2013). The Kyoto Protocol used GWP with a time horizon of 100 years.

Emissions metrics have normally been calculated for global emissions. However, for SLCFs, due to their short lifetimes compared to large-scale atmospheric mixing times, and because the chemistry and radiative effects on climate depends on the regional physical conditions, even the global mean radiative forcing depends on the region of emissions (Fuglestad et al., 1999; Wild et al., 2001; e.g., Berntsen et al., 2005; Naik et al., 2005). Then, the emission metric values will vary for different emission locations (Fuglestad et al., 2010). In addition, ~~a~~-distinct patterns in the temperature response appear from all forcings (Boer and Yu, 2003; Shindell et al., 2010). A growing literature investigates how the weights of the emission metrics change as emissions from different regions of the world are considered. Collins et al. (2013) assessed variations in emission metrics for four different regions (East Asia, Europe, North America, and South Asia) for aerosols and ozone precursors, based on radiative forcings from consistent multimodel experiments from the Hemispheric Transport of Air Pollution (HTAP) experiments given by Yu et al. (2013); Fry et al. (2012). Collins et al. (2010) investigated also how emission metric values differ between regions, including vegetation responses. Bond et al. (2011) quantified differences in RFs for BC and OC emissions from different locations and types of emissions.

For SLCFs, the impact also depends upon the season of emission~~of emissions depends also on the seasons~~. As the chemistry and radiative effects vary between summer and winter, the RF per unit emissions will differ between the seasons. An additional factor is that the magnitude of emissions fluctuates between the seasons, which can also be the case for LLGHGs. E.g., emissions of certain species from wood burning for domestic heating will be much larger in winter than summer (Streets et al., 2003).

Bellouin et al. (2016) detail a comprehensive set of dedicated RF calculations with four models (ECHAM6-HAMMOZ, HadGEM3-GLOMAP, NorESM and OsloCTM2) for emission perturbations in different regions (Europe, East Asia, shipping, as well as global) and seasons (NH summer (May-Oct) and winter (Nov-Apr)) for various SLCFs or their precursors (BC, OC, SO₂, NH₃, NO_x, CO, and VOC) and for global annual emissions of CH₄. Here, we present separate emission metric values for emissions during NH summer and winter emissions. In this study, we use the RF results from Bellouin et al. (2016) to calculate emission metrics for the different regions and seasons. We produce emission metrics for standard pulse emissions, but also for an emission profile consisting of a ramped-up period of 15 years followed by a sustained case, which can illustrate a gradual implementation of technology standards. As the study is based on several models running the same experiments, this data allows us to investigate the robustness in our findings. We analyze the robustness for individual species, as well as for hypothetical policy mitigation packages. Finally, we discuss how the emission metrics presented here can be used in mitigation policies.

2. Material and methods

2.1 Radiative forcing

An overview of the 4 different coupled-chemistry climate models or chemical-transport models presented by Bellouin et al. (2016), their resolution and species investigated (SO₂, BC, OC, NH₃, NO_x, CO, VOC, and CH₄) is given in Table 1. Not all models have calculated RF for all species. While all four

models give RFs for BC, OC, and SO₂, only the OsloCTM2 calculated RF for NH₃. Three models (OsloCTM2, HadGEM3, NorESM) have calculated RFs for the ozone precursors and CH₄.

The calculations are based on different processes that affect RF, see Bellouin et al. (2016). For aerosols and aerosol precursors, all four models calculate the aerosol direct and 1st indirect (cloud-albedo) effect, except ECHAM6 which only diagnosed direct RF. For BC, OsloCTM2 estimated in addition the RF from BC deposition on the snow and semi-direct effect. Only a few previous studies, such as Bond et al. (2013), have included the semi-direct effect in emission metrics. For the ozone precursors and CH₄, the total RF consists of the aerosol direct and 1st indirect effects, short-lived ozone effect, methane effect, and methane-induced ozone effect. Only OsloCTM2 includes nitrate aerosols, but nitrate aerosol RF has been used to complement the estimates by other models.

The best estimate of a species' RF is given as the sum of all the processes, in which the average across the models is used for each process. ~~Not all processes, nor species, have been modeled by all models, and hence, the average for a process can be based on anything from only one model to four models.~~ ECHAM6 is not included in the best estimate for BC, OC₂ and SO₂, since this model does not diagnose the 1st indirect effect. The best estimate is based on only the OsloCTM2 model for BC deposition on snow and BC semi-direct effect, while the best estimate are based on three models for all other processes (aerosol effects, short-lived ozone, methane, and methane-induced ozone). ~~As this 1st indirect effect is significant compared to the direct effect in OsloCTM2 and NorESM for OC and SO₂, but to a much smaller degree for BC, we exclude ECHAM6 for the OC and SO₂ averages, but not for the BC average.~~

For the high and low estimate, we sum the highest and lowest value, respectively, for each individual process.

These global-mean RFs of various species were calculated for emissions in different regions. The three regions, following tier 1 HTAP regions, are Europe (Western and Eastern Europe up to 66°N including Turkey), East Asia (China, Korea, and Japan), and the global shipping sector. RF values are also available from remaining land areas outside of Europe and East Asia; ~~for which results~~ for this case are presented ~~for~~ in SI Sect. 1. Values for global emissions were also utilized. Emissions from shipping are not included in the global estimates since only OsloCTM2 and NorESM include detailed estimates for the shipping sector. All estimates are given for Northern Hemisphere (NH) summer and NH winter. As emissions globally and from the shipping sector occur in both hemispheres, the two seasons are a mix of summer and winter conditions. For these two cases, we refer to NH winter and NH summer.

2.2 Emission metrics

In this study, we use the emission metrics GWP and GTP with varying time horizons. In all perturbations, RF is annually and globally averaged, thus, the responses are also annually averaged. AGWP for species *i* at time horizon *H* is defined as

$$AGWP_i(H) = \int_0^H RF_i(t) dt, \quad (1)$$

where RF is the time varying radiative forcing following a unit mass pulse emission at time zero. The calculations of the RFs build on the framework previously shown for short-lived ozone depletion gases for the metric the Ozone Depletion Potential (Olsen et al., 2000; Bridgeman et al.,

2000;Wuebbles et al., 2001). This work led to the mathematical relationship between the steady-state impacts from sustained emissions, the pulse response function, and the steady-state lifetime (Prather, 2002), which we follow in our RF calculations. For aerosols, the radiative forcing values (RF_{ss}) ($W\ m^{-2}(kg\ yr^{-1})^{-1}$) calculated by Bellouin et al. (2016) are based on assuming that the emissions are sustained for a year and hence the concentrations are close to equilibrium values because of their short steady-state lifetimes. These RF_{ss} values have been converted into RF values ($W\ m^{-2}\ kg^{-1}$) for an instantaneous emission for BC, OC, SO_2 , and NH_3 by the formula (Aamaas et al., 2013):

$$RF \approx \frac{RF_{ss}}{\tau}, \quad (2)$$

where τ is the perturbation lifetime (yr) of the aerosol species. This conversion is only applicable when the adjustment time of the species is significantly less than one year. The adjustment time can be dependent on different processes with different timescales, such as wet and dry deposition. The perturbation lifetimes are model specific and given in Bellouin et al. (2016).

The AGTP is given as

$$AGTP_i(H) = \int_0^H RF_i(t) IRF_T(H-t) dt, \quad (3)$$

where $IRF_T(H-t)$ is the impulse response function for temperature~~temperature response~~ at time H to a unit radiative forcing at time t . The equations for the AGTP calculations for aerosols and ozone precursors are given in Aamaas et al. (2013). These emissions metrics (AGWP, AGTP) are given in absolute forms. They can be normalized to the corresponding effect of CO_2 , where M is GWP or GTP, given as

$$M_i(t) = \frac{AM_i(t)}{AM_{CO_2}(t)}. \quad (4)$$

To calculate the time-varying RF for a pulse emission of CO_2 an impulse response function (IRF_C) for CO_2 is needed. Here we use the IRF_C based on the Bern Carbon Cycle Model (Joos et al., 2013) as reported in Myhre et al. (2013). The IRF_T is here treated independently of the emitted species and based on simulations with the Hadley Centre CM3 climate model (Boucher and Reddy, 2008). These parameterizations have uncertainties, and Olivié and Peters (2013) studied the effective of different IRF_T from different atmosphere-ocean general circulation models and found that the uncertainty is the largest for the most short-lived SLCFs.~~the spread due to IRF_T is larger for SLCFs than for species with longer lifetimes (Olivié and Peters, 2013)~~ The emission metric parameterizations for CH_4 comes from Myhre et al. (2013).

Emission metrics for pulse emissions are in principle the most useful metrics, even though emissions follow a given temporal profile. A pulse can be seen as an instantaneous emission, or constant emission during a short period ($\ll H$), followed by no emissions. In real life, implementing mitigation can be a gradual process where emissions are gradually reduced over some period, followed by a sustained level of emission reduction. This reflects regulations or technical improvements that are phased in over a given period and then sustained indefinitely. Such an emission profile, or mitigation

profile, can be called a “ramping-up”. These different types of emission profiles are shown in Fig. 1. For ramping-up or any other emissions scenarios, the emission metric can be calculated by a convolution. A temperature response is calculated as

$$\Delta T_i(t) = \int_0^t E_i(t') AGTP_i(t-t') dt' \quad (5)$$

E is the emission scenario and AGTP gives the temporal temperature perturbation for a unit of emissions. The absolute metrics for compound i for the ramping-up scenarios (AM_i^R) are calculated according to

$$AM_i^R(H) = \sum_{t_e=0}^H E_i(t_e) \times AM_i^P(H-t_e), \quad (6)$$

where $AM_i^P(H)$ is the corresponding absolute pulse metric (e.g., AGWP or AGTP) for time horizon H, and $E(t_e)$ is the emission at time t_e . The integral in Eq. 5 is the general notation, while we apply this in our calculations with the sum in Eq. 6. Note that the sustained case is a special case where $E(t)=E_s$ for all t. For a ramping-up period of mitigation of TH years, change-in-emissions in year t in the first

TH years are $E(t_e) = \frac{t_e \times E_s}{TH}$ and after that E_s . We show results only for a ramping-up period of

TH=15 years, but we have also investigated other implementation rates. The total response for a scenario is found by multiplying Eq. 6 with the total emission change. Note that since emission metric values for SLCFs increase with decreasing time horizon (because they are short lived), their “ramping-up” emission metrics values are significantly higher than the standard pulse based values.

Emission metrics normalized to the corresponding absolute emission metric for ramping-up emissions of CO₂ ($M_i^R(H)$) are calculated by

$$M_i^R(H) = \frac{AM_i^R(H)}{AM_{CO_2}^R(H)}. \quad (7)$$

Note that since the pulse metrics are given by region and season, so are the ramping-up metrics ($M_i^R(H)$).

For policymakers to apply this concept to compare different (n) sets of mitigation options (all following the same ramping-up profiles over time, but with different mix of species, regions, and seasons) the net impacts ($I_n(H)$) (i.e., AGWP or AGTP) for all options must be calculated according to

$$I_n(H) = \sum_j \sum_i \Delta E_i(j) \times M_i^R(H). \quad (8)$$

Here $\Delta E_i(j)$ denotes the total mitigation (e.g., at the end of the ramping-up period) of component i emitted in region j .

3. Results

3.1 Emission metric values

3.1.1 Best estimates

First, we present the best estimate of emission metric values for pulse emissions, see Table 2 for GTP(20) values. Additional values for GWP and for other selected time horizons are given in Table SI1. Due to space constraints, we can only present values for a few time horizons. ~~The choice of~~What emission metric and time horizon ~~to use~~ depends on the application, and a range of different justified choices are possible (e.g., Aamaas et al., 2013). If the focus is on temperature change in the next few decades, GTP(20) ~~is appropriate~~can be applied. In Fig. 2, GTP(20) values are given for the different species, decomposed by a range of processes. Figure 3 presents results for GWP(100) for the ozone precursors. We first focus on a few selected time horizons, but Sect. 3.1.5 shows how emission metrics evolve for a range of time horizons.

The uncertainties in Fig. 2 and Fig. 3 are given as the range across all contributing models. The uncertainty is in general larger than the variation between different regions and seasons. Thus, when including the uncertainty, it is less clear which region and season give the largest and smallest emission metric values. However, we will show in Sect. 3.1.3 and 3.1.4 that the best estimate is more robust than the uncertainty bars indicate.

The emission metric values for the shipping sector are based on only two models (OsloCTM2 and NorESM). We do not provide uncertainty ranges for shipping due to the low numbers of models. Further, the robustness of these values presented is lower than for the other regions for the same reason.

We find distinct differences between regions and seasons for all species. For the aerosols BC, OC, and SO₂, the magnitude of the total GTP(20) values are higher for emissions during summer than winter and larger for Europe than for East Asia. ~~However, the emission metric value for winter emissions of BC is only slightly higher for Europe than for East Asia. The higher emission metric values for Europe than for East Asia is likely caused by a more polluted baseline in East Asia, which leads to a saturation for some of the interactions.~~ Collins et al. (2013) also estimated higher values for Europe than East Asia, while Fuglestad et al. (2010) based on earlier calculations in the literature gave partly conflicting results. As a significant share of the emissions from the shipping sector, as well for global emissions, are occurring in the Northern Hemisphere, the seasonal variation is similar for these two categories except for BC for shipping. Seasonal variations are mainly driven by aerosol RF, which is mainly located in the shortwave spectrum. Greater sunlight duration in local summer yields stronger RFs (Bellouin et al., 2016). Seasonal differences in atmospheric lifetimes, caused by seasonality in precipitation, will also contribute.

For BC, the elevated aerosol ~~direct~~ effect in summer is partially cancelled out by a cooling effect by the semi-direct effect (see Fig. 2). The semi-direct effect is due to the absorption of solar radiation of

particles, which affects the atmospheric static stability, and impacts on clouds. The impact of BC deposition on snow is largest for emissions during winter and larger for Europe than East Asia. The BC surface albedo effect is governed by the extent of snow and ice covered surface areas, but depends also on the availability of solar radiation where the BC is deposited. For Europe, the snow effect is 5465% of the direct effect in winter and 2.63-1% in summer, while the corresponding percentages are 2226% and 1.14-5% for East Asia. The shares are similar for the shipping and global, with lowest shares for global emissions. As explained by Bellouin et al. (2016), this is due to atmospheric transport: according to the models, European emissions of BC are preferentially transported to the Arctic, where they modify the albedo of snow. Seasonality is driven by snow cover, which is larger in winter and early spring. In Europe, the semi-direct effect is -38-32% of the direct effect in summer and -9.5-3.3% in winter, while it is -42-51% and 4.414%, respectively, for East Asia. As the other regions are a mix of summer and winter because both hemispheres are included, the semi-direct effect is smeared out ~~on-over~~ the two seasons, but largest in absolute value for NH summer. For NH₃, the GTP(20) value is larger for Europe than East Asia, in summer but not for winter, as explained by Bellouin et al. (2016). Ammonium nitrate aerosol formation is strongly dependent on relative humidity and temperature, and competes for ammonium with ammonium sulphate aerosols, which has larger concentrations in local summer (Bellouin et al., 2011). Those complex interactions may explain different seasonalities in different regions, and will contribute to model diversity.

For the ozone precursors, the variability between regions and seasons is smallest for CO. For CO, GTP(20) values are higher for winter than summer. Due to the longer lifetime of CO during winter, a large fraction of the CO emitted during winter will undergo long-range transport and will be oxidized in relatively clean low-NO_x environments. There CO-oxidation will reduce OH and thus increase the methane lifetime. As can be seen in Fig. 2, it is the indirect methane effect that leads to higher metric values for wintertime emissions. Furthermore, GTP(20) values of CO are slightly larger for East Asia than Europe. For VOC, the seasonal variability is opposite with highest GTP(20) values for summer. Further, GTP(20) values are higher for Europe than East Asia. The overall picture is a bit more complex for NO_x. The seasonal difference is very small for GTP(20) values in East Asia. However, for Europe, the GTP(20) value is more negative for summer and less negative for winter. Shipping has the largest GTP(20) values in magnitude for all ozone precursors, especially the driven by a large methane effect, driven by the relatively clean atmospheric conditions around the emission locations. The models may overestimate the ozone production of NO_x emissions from shipping, as they do not represent ship plumes, but assume instantaneous dilution of emissions in the grid boxes (Paoli et al., 2011). Collins et al. (2013) observed the same annual pattern for Europe and East Asia as we do. One notable feature for NO_x is that the aerosol effect is negative for all cases except for shipping, mainly because the values for shipping are based on two models and the other values are based on three models. The positive value for shipping is the average of two models with opposing signs; thus, there is significant uncertainty in the best estimate. This model disagreement for NO_x is discussed in detail by Bellouin et al. (2016).

For aerosols emissions and the major aerosols precursors, the relative ratios between the different regions and seasons are constant while varying the emission metric and time horizon applied. On the other hand, the relative ratios between different emission metric values for the ozone precursors differ with varying emission metrics and time horizons. The ratios for the aerosols are fixed since the aerosols have little effect on perturbations of atmospheric composition and components with long adjustment times. By contrast, the ozone precursors affect processes with longer time constants. By

causing a change in OH-levels, methane with an adjustment time of about 10 years is perturbed. Hence, we also show GWP(100) values for the ozone precursors (Fig. 3), while similar figures for the other species are provided in SI (Fig. SI1). For the ozone precursors, the aerosol direct and indirect effect and the short-lived ozone effect are given relatively more weight for GWP(100) than GTP(20) than the methane effect and methane-induced ozone effect, since GWP integrates the RF up to the time horizon, while GTP is an end-point indicator. As the time horizon increases, the relative contribution from methane and methane-induced ozone increases and the contribution from aerosols and short-lived ozone decreases. The overall picture presented here for GTP(20) and GWP(100) is mostly similar. But for NO_x, no significant seasonal difference was observed in GTP(20) values for East Asia, the value in winter is almost twice as negative as the summer values for GWP(100). For shipping emissions in NH summer, the emission metric value changes from clearly negative for GTP(20) to almost zero for GWP(100).

We provide only one global emission metric value for CH₄, as CH₄ emissions are relatively well-mixed in the atmosphere and expected differences due to regionality and seasonality are small (Bellouin et al., 2016). The aerosol effect is weakly positive, while the models give a wide range from weakly negative to strongly positive, as discussed in Bellouin et al. (2016).

3.1.2 Comparison with literature

As already ~~observed~~noted, the variations with respect to regional emissions for emission metric values are in line with Collins et al. (2013). Fuglestad et al. (2010) also presented emission metrics with respect to regional emissions based on earlier calculations in the literature, but with some conflicting results between available studies. Due to this spread, oOur findings are partlytherefore somewhat in line with Fuglestad et al. (2010). In general, the specific emission metric values are also comparable with Collins et al. (2013). However, a complete comparison is not possible as we have included the effect of aerosols for the ozone precursors and the semi-direct and deposition on snow effect for BC. The findings are also generally similar to previous estimates for emission metrics of global emissions (e.g., Fuglestad et al., 2010), with some discrepancies we will discuss here. A comparison of modeled GWP and GTP values with a selection from the literature for some selected time horizons is given in Table SI1.

For BC, Bond et al. (2013); Bond et al. (2011) presented about ~~20-40~~50-60% higher emission metric values (GTP and GWP), while other studies (Fuglestad et al., 2010; Collins et al., 2013) are in line with or up to 40% lower than this study and Hodnebrog et al. (2014) give significant lower values. As discussed in Hodnebrog et al. (2014), the atmospheric lifetime of BC may be shorter and the BC emissions may be larger than previously thought (e.g., Fuglestad et al., 2010) leading to emission metric values almost halved compared to previous estimates (-44% for the example given in Hodnebrog et al. (2014)). The OC values in our study are more than~~almost~~ 200% higher in magnitude than the literature, driven by the high values in one of the models (NorESM). The OC values from NorESM are driven by a strong indirect effect. When this indirect effect is excluded, the NorESM value is similar to the others as well as the literature. For SO₂, the emission metric values for the winter season are similar to or up to 60% stronger than the literature, while they are more than doubled for summer. As for OC, the more negative emission metric values for SO₂ are driven by the inclusion of the indirect effect. The one study (Shindell et al., 2009) we found on NH₃ gave emission metric values that are about the double of our annual average. The literature shows a wide range in the emission metric values for NO_x depending on the source and region. Our estimates are within this

range but, on the more negative side within the range, about 80% stronger than the values used for land-based emissions in Myhre et al. (2013). The emission metric values for CO are roughly 0-30% higher than in the literature, partly driven by the additional positive impact of including the aerosol effect. For VOC, the emission metric values are roughly the double or more than those found in the literature, even with a negative contribution from the aerosol effect (Bellouin et al., 2016). The emission metric values for CH₄ are mostly lower than those in Myhre et al. (2013) (29% and 19% lower for GTP(20) and GWP(100), respectively), mainly due to a shorter methane atmospheric lifetime, as well as a smaller contribution from the indirect effect on ozone.

3.1.3 Robustness for individual species

The differences in the emission metric values between the emission regions and seasons of emissions, seen for the best estimate holds generally in each model, which strengthens our confidence in the modeled variations between regions and seasons. For emissions of aerosols and their precursors, the magnitude of GTP(20) values is higher in summer than winter in ~~8688~~ % of the model cases ~~and another 8% are marginally the other way~~. The consistency between the individual models and our best estimate based on the models is 100% for SO₂. The metric values for European emissions are larger in magnitude for most cases than East Asia. In summer, this is true for 92% of the cases and ~~5058~~ % in winter in addition to ~~3317~~ % that are marginally the opposite. Yu et al. (2013) also observed that the regional dependency in RF was robust for a number of models with the same regional pattern as in our study.

For the ozone precursors, the variation in GTP(20) values observed for the best estimate also holds for most of the models. For both regional and seasonal variability, 83% of the model cases agree with the best estimate. For CO, all cases agree that the GTP(20) values are larger for East Asian emissions than European emissions and for winter than summer, even though the relative differences in GTP(20) values between Europe and East Asia in summer and winter are relatively small. The difference may occur since the East Asia region is located closer to the Equator. The findings for NO_x and VOC are also relatively robust, where the model cases agree ~~7583~~ % for NO_x and ~~8367~~ % for VOC. The same tendencies in the regional pattern were also found by Collins et al. (2013).

3.1.4 Robustness in total climate impact

Emission metrics are used to quantify the climate impacts of different sets of emission changes following either mitigation policies or changes caused by some other mechanisms (e.g. technological development). However, the uncertainties given by the model ranges for individual regions, seasons and species shown in Fig. 2 and Fig. 3 do not provide a good indication for the robustness of the *total* impacts estimated by the emission metrics, because there might be significant correlations between species. By robustness here, we mean how uncertain is the total climate impact of a given set of emission changes (changes of multiple species, seasons and regions) and related to this how robust would a ranking (in terms of net climate impact) of possible mitigation measures be, given the individual uncertainties shown in Fig. 2 and Fig. 3.

Models with more efficient vertical transport and/or slow removal of aerosols by wet scavenging will tend to give longer lifetimes for the aerosols and thus stronger RF per unit emission for all aerosol species, and thus emission metric values for the individual species and seasons would be correlated. This means that the ranking of measures and the net impact of measures that lead to reduction in emissions of co-emitted species that cause a cooling effect could be more robust. Similar effects can

be expected across ozone precursors due to non-linear chemistry effects and removal efficiencies; for instance, such correlations across models were observed for the climate effect of NO_x emissions from aviation by Holmes et al. (2011). To investigate this we first focus on the correlation. To put all species on a common scale we calculate the normalized variability (across species, regions and seasons) for the best estimate (NV_{BE}) and for the individual model estimates (NV_m)

$$NV_{BE}(r,s,i) = \frac{M_{BE}(r,s,i) - M_{BE,min}(i)}{M_{BE,max}(i) - M_{BE,min}(i)}, \quad (9)$$

and

$$NV_m(r,s,i) = \frac{M_m(r,s,i) - M_{BE,min}(i)}{M_{BE,max}(i) - M_{BE,min}(i)}. \quad (10)$$

$M_{BE}(r,s,i)$ denotes the best estimate for the emission metric value for species i , region r and season s , while $M_m(r,s,i)$ denotes the emission metric value from a single model m for species i , region r and season s . $M_{max}(i)$ is the maximum GTP(20) value found in any region (Europe, East Asia, and global) and season (NH summer and winter) for species i , while $M_{min}(i)$ is the minimum value.

The values of NV_{BE} are numbers between 0 and 1. As GTP(20) values from individual models can be larger than the maximum from the best estimate and smaller than the minimum, $NV_m(r,s,i)$ can be larger than 1 or negative, respectively. Figure 4 is a scatter plot between NV_{BE} and all the individual NV_m values, where the colors indicate model and shapes of the symbol indicate component. Since the processes that could lead to correlations are somewhat different for aerosols and ozone precursors (e.g. non-linear chemistry effects for the latter) the species are split into two separate panels.

Figure 4 clearly shows the correlation between the species for the individual model emission metrics. For the aerosols, HadGEM and ~~particularly~~ NorESM tend to give higher (in absolute terms, i.e. more negative for cooling agents) emission metric values compared to the best estimate, while ECHAM gives much lower values. For the ozone precursors, the picture is the opposite, with NorESM being lower than the BE while the OsloCTM is higher. This indicates that for both aerosols and ozone precursors there are generic features in the models related to representation of key processes (e.g. vertical mixing, wet scavenging, ozone production efficiency etc.) that systematically affects the emission metric values.

These correlations between the estimates for the individual species have to be taken into account when the uncertainty in the net effect of a multi-component mitigation policy is estimated. Since different SLCFs are often co-emitted, most mitigation options will affect emissions of several species at the same time. The uncertainty in the estimate of the net effect depends on the composition of the mitigation, i.e. mix of species, regions, and sectors. To be useful for policymaking, the emission metrics should be robust enough so that there is trust in the sign of the net effect of a mitigation measure and that the uncertainty in the emission metrics does not hinder a ranking of different measures when cost-efficiency is considered. Figure 5 shows the estimates of the net effect (here in terms of temperature change after 20 years, i.e. using AGTP(20) for pulse emissions) when using the sets of emission metrics from the individual models. First, we consider a global mitigation of a 10% reduction in emissions of all SLCFs for which the best estimate is positive for the AGTP(20) (BC, OC, and VOC – labelled B on Fig. 5), and then a 10% global reduction of all SLCFs (an extreme case of also

reducing the co-emitted cooling species OC, SO₂, and NO_x— case A on Fig. 5). The shipping sector is not included in this sensitivity test as the best estimate is only based on two models. ECHAM6 did not calculate RFs for the ozone precursors, therefore, values for the best estimate is given for those species. NH₃ is not included, as only OsloCTM2 provided RF estimates of that. These scenario estimates are based on emission inventories for 2008 (Klimont et al., In prep.). For a 10% reduction in emissions of the warming SLCFs (BC, CO, and VOC), the best estimate gives a global reduction in temperature of 0.610-55 mK 20 years after a pulse, with a spread of -0.38-0.39 to -0.85-0.83 mK. When the cooling components are included, the best estimate gives a global warming of 0.490-48 mK, with models ranging from 0.060-05 to 0.490-46 mK. Hence, all models agree that a reduction of those six SLCFs will cause warming, but for onetwo of the models there is only a marginal warming.

The black bars in Fig. 5 give the uncertainty in the net global temperature effect assuming all the metric values are independent. This gives a similar or narrower uncertainty interval than the spread of the estimates using the individual model metrics, again showing that there is considerable correlation ~~between~~ in the model estimates. However, if the difference between the models were 100% systematic (i.e. one model always giving the lowest estimates by magnitude and another model giving the highest), then the model based interval would be given by the blue bar in Fig. 5. From this analysis, we conclude that the uncertainty for an estimate of the net temperature effect of multi-component emission change is enhanced due to the correlations; however, for mitigation measures that mainly change emissions of species with positive GTPs, the sign of the global temperature signal is robust.

Since not all processes are included in all the models, the average of all models in Fig. 5 will differ from the best estimate. This deviation is observed in both scenarios, but clearest for a mitigation scenario including both warming and cooling SLCFs, as the net climate impact is a sum of large positive and negative numbers. The processes not included are dominated by cooling. Three out of four models do not include the cooling from the semi-direct effect of BC, as well as the mainly cooling from nitrate for the ozone precursors and SO₂. As a consequence, the individual models tend towards more cooling or less warming than the best estimate for a mitigation scenario of SLCFs.

Our findings show that the robustness is largest for individual species, i.e., what region and season of emissions to mitigate for an individual species. Next follows a subgroup of species that correlates, such as aerosols. Lowest robustness is given for mitigation for all SLCFs. However, we observe that all models agree whether two hypothetical mitigation scenarios give warming or cooling.

3.1.5 Variations with time horizon

We have until now presented emission metric values at certain fixed time horizons; however, these values vary greatly with time horizon, which is partially controlled by CO₂. SLCFs impact the atmosphere for a short time, as aerosols and aerosol precursors have atmospheric lifetimes of about a week. Methane, however, has an atmospheric perturbation lifetime of about 12.4 years (IPCC, 2013). Due to the inertia in the climate system, the climate is impacted for at least 10-20 years from a radiative forcing lasting only a week (Peters et al., 2011; Solomon et al., 2010; Fuglestad et al., 2010). The denominator in the emission metrics is CO₂, which impact the atmosphere for centuries (IPCC, 2013). However, aerosols are very strong at perturbing the radiative balance of the Earth while they are situated in the atmosphere; for instance, the radiative efficiency ($Wm^{-2} kg^{-1}$) of black carbon is about a million times larger than the radiative efficiency of CO₂. Thus, the magnitude of the

normalized emission metric values is very high for short time horizons, but decreases rapidly with increasing time horizon. The aerosols have the highest emission metric values in magnitude for the shortest time horizons, see Fig. 6 and Fig. 7 for GTP and GWP values in the first 50 years after a pulse emission. Additional figures are provided in the SI. NO_x often has a positive emission metric value for the first 5-10 years, followed by negative numbers, as the sum of the short-lived effects are positive and the longer lived effect negative. However (see Fig. 7), we find cooling already from year one for emissions in Europe during all seasons and East Asia during winter as the cooling from the aerosol effect is as large as or larger than the short-lived ozone effect. This aerosol effect is cooling for all regions, while the models disagree about the impact for shipping. The results for the shipping sector should be considered with care as the best estimate is based on only two models with large inter-model variability-except shipping. The time dimension is especially important for NO_x and the other ozone precursors, as different regions and seasons are given different weights with different time horizons. For instance, shipping in summer has most positive GTP values for NO_x of all cases in the first 10 years, but becoming the second most negative after 20 years. For a specific region and season, the weighting between the aerosols and ozone precursors is also changing with variable time horizon.

3.2 Global temperature response

We have applied the emission metrics on an emission dataset for year 2008 (Klimont et al., In prep.). The variability discussed in the previous section is also found in the global temperature response for regional and seasonal emissions (Fig. 8). A seasonal profile is included in the emissions, with typically largest emissions in the winter season, but the temperatures should be taken as being annual mean values. As for the emission metric GTP, tThe temperature response drops rapidly off due to the short lifetimes of the SLCFs. In general, the total temperature response is governed by the SO₂ emissions. Hence, the total climate impact is a cooling for all regions and seasons, but largest for emissions in summer. The emission mix is different between the regions. For instance, SO₂ and NO_x generally dominate for shipping. Europe and East Asia have a broader mix of SLCFs that impact the climate. The temperature perturbation, dominated by cooling, is in agreement with Aamaas et al. (2013), who also showed that the warming from global emissions of CO₂ is larger than the net cooling from the SLCFs after only 15 years. We have presented the global temperature response, while regional variations will occur beyond this global mean response (e.g., Lund et al., 2012).

3.3 Gradual implementation of mitigation

We have calculated emission metrics for pulse emissions, which is the standard method~~typical way of presentation~~. However, changes in emissions are often gradual in real life. In this section, we present how the emission metric values differ based on a gradual implementation of mitigation policy (see Fig. 9), which is calculated by convolution as given in Eq. 2.6. We show results only for a ramping-up period of 15 years, but we have also looked at other implementation rates. The emission metric values presented here are for Europe in the summer season, with the exception of CH₄ which for illustrative reasons apply the. ~~We complement with emissions of CH₄, based on~~ parameterizations in Myhre et al. (2013).

For species that have a shorter influence on the climate system than CO₂, the normalized emission metric values will almost always be larger in magnitude for sustained emissions than pulse emissions. The only exception is for species with competing-counteracting processes on different timescales, such as for NO_x in Fig. 9. The 15-year rampinggrowth scenarios give slightly higher normalized emission metrics than the sustained case (again with the exception of NO_x at short time horizons),

but those emission metric values approach each other in the long term. The longer the ramping-up period lasts, the larger the emission metric value becomes, but the value converges to the sustained emission case for time horizons beyond the ramping-up period. The normalized emission metric values are higher in the growth-ramping scenarios than the sustained case since the impact of the shorter lived effects are given more weight than CO₂ which is undergoing the same ramping scenario. Hence, a mitigation scenario that will have a gradually increasing effect over several years will, for most species, have a higher metric value than for mitigation that instantly takes effect. What this means is that one obtains the benefit of mitigating SLCFs (i.e., higher CO₂ equivalent emission reduction and thus higher value on an emission trading market or in a cost-effectiveness analysis) as soon as those reductions begin now. The reason is the planned emission reductions of the shorter lived species close to the time horizon has a large impact. Hence, these emission metrics for ramping-up scenarios should be used with care. If there is a chance that the emission reductions are reversible and will not be kept in place (or replaced by even stronger reductions) until the time horizon, the ramping-up metrics will overestimate the effects.

We also present the temporal evolution for all the regions and seasons for BC and NO_x in Fig. 10, while Fig. 9 only showed these emission metric values for Europe in summer. While the regions and seasons are ranked the same for all time horizons for the aerosols, the ranking may differ for the ozone precursors for different emission metrics and different time horizons due to competing processes on different timescales, especially for NO_x.

The other significant difference between emission metrics based on pulse and ramping-up emissions is the sign switch for NO_x (see Fig. 79). In the pulse case, the GTP values are negative or turn negative within the first 6 years for all cases except summer shipping when it takes 10 years, with NO_x from shipping during summer taking 10 years. The sign switch is much slower for the ramping-up scenario emission metrics. Even after 10 years, half5-out of the -8 cases give positive GTP values (see Fig. 10). In the long run (>22 years), all the GTP values with the exception of shipping in summer, are negative. Thus, if a time horizon of 10 years is picked, the mitigation policies of NO_x will depend highly on the assumed emission scenario.

3.4 Policy implications

Emission metrics can be applied as an “exchange rate” between different emissions in climate policies, such as for different LLGHGs in the Kyoto Protocol. While the calculations of how emissions impact the climate build on scientific knowledge, how to use the emission metrics is given by political choices. There is no particular reason why there should be one and only one goal for our climate policy (Fuglestad et al., 2000; Rypdal et al., 2005; Daniel et al., 2012; Sarofim, 2012; Jackson, 2009; Victor and Kennel, 2014). In particular there may be harmful impacts of exceeding a long-term temperature constraint (e.g., 2°C), while at the same time there is more immediate concern about short term effects over the next decade or so. The rationale behind a climate policy focusing on SLCFs must be that there are potential harmful effects of climate change over the next few decades. However, CO₂ and other LLGHGs should also be included in evaluation of possible mitigation measures under a short-term goal as these species also influence the climate on short timescales. Historically, emission metrics within international climate policy have been applied to emissions of LLGHGs. However, as the uncertainty for the emission metrics of SLCFs is reduced and the values become more robust, this opens up for regimes that also include non-methane SLCFs beyond CH₄, e.g., CCAC. Recently, Mexico included BC in their Intended Nationally Determined Contribution (INDC)

submitted to the UNFCCC (Mexico, 2015). But as pointed out by Allen et al. (2016) a generic 'CO₂-equivalent' emission reduction target by a given year, defined in terms of GWP(100) and containing a substantial element of SLCF mitigation, represents an ambiguous commitment to future climate.

A general difference between LLGHGs and SLCFs is that the location of the LLGHG emissions does not matter, while we have shown that different locations, as well as timing of emissions, will cause different impacts of SLCFs (Fuglestvedt et al., 1999; Naik et al., 2005; Berntsen et al., 2006; Shindell and Faluvegi, 2009; Berntsen et al., 2005). In addition to differences in the total global response, the spatial distribution of the impact depends on the location and timing of the SLCFs emissions. Further, we have shown that individual models may give significantly different emission metric values than other models.

4. Conclusion

We have presented emission metrics for regional emissions of several SLCFs (BC, OC, SO₂, NH₃, NO_x, CO, and VOC) based on four different models. We have focused on the emission regions Europe and East Asia, but also given numbers for the global shipping sector and total emissions from all countries. Values have been estimated for emissions in both the summer and winter seasons. For the aerosols, the magnitude of the emission metric values is larger for Europe than East Asia and for summer than winter. The variability between the models is generally larger than the variations between regions and seasons. However, most models agree that specific regions and seasons have larger emission metric values than others. Hence, the robustness of this ranking is better than can be interpreted from the variability between models. The co-variability between models is also seen for the ozone precursors. For CO, the emission metric values are larger for East Asia than Europe and for winter than summer. The pattern is the opposite for VOC with larger emission metric values in Europe and in summer. NO_x is more complex with more negative values in summer than winter for Europe. In East Asia, we model no significant difference between the seasons for GTP(20) for NO_x, while the GWP(100) for winter emissions is more negative.

We have also calculated emission metrics for transient scenarios where we consider a ramping-up of the emission over time. This emission metric will better represent the effect of imposing a mitigation measure (i.e. a new technology standard) that is known to give a long term change of emissions. For species that have a shorter influence on the atmosphere than CO₂, the magnitude of the emission metric value is larger for a mitigation scenario with a gradually increasing effect over several years than for the standard pulse based emission metric. The only exception is species that have competing short and longer lived effects that are positive and negative, notably for NO_x.

We observe variability in the emission metrics between different regions and seasons, however, with varying robustness between the models. As the certainties in the numbers increases, the regional and seasonal differences may be accounted for in mitigation policies, agreements and potential trading schemes involving SLCFs. One robust finding in our study is that, per unit mass of emissions, emissions of aerosols and their precursors in Europe should likely be given more weight than emissions in East Asia, as well as emissions in summer likely more weight than in winter. When emission metrics are applied, the selection of the specific emission metric and time horizon is of significance. The emission metric values for SLCFs drop quickly with time horizon. For the ozone precursors, the ranking between different regions and seasons can vary with different time horizon. Thus, emission metrics must be used based on careful consideration of these factors.

Acknowledgements

The authors would like to acknowledge the support from the European Union Seventh Framework Programme (FP7/2007-2013) under grant agreement no. 282688 – ECLIPSE, as well as funding by the Norwegian Research Council within the projects “Climate and health impacts of Short-Lived Atmospheric Components (SLAC)” and “the Role of Short-Lived Climate Forcers in the Global Climate Regime” (project no. 235548). We thank Øivind Hodnebrog and Dirk Olivié for providing radiative forcing data and Glen Peters for comments. We thank two anonymous referees for valuable comments that improved the paper, and the editor.

References

- Aamaas, B., Peters, G., and Fuglestad, J. S.: Simple emission metrics for climate impacts, *Earth Syst. Dynam.*, 4, 145-170, 10.5194/esd-4-145-2013, 2013.
- Allen, M. R., Fuglestad, J. S., Shine, K. P., Reisinger, A., Pierrehumbert, R. T., and Forster, P. M.: New use of global warming potentials to compare cumulative and short-lived climate pollutants, *Nature Clim. Change*, advance online publication, 10.1038/nclimate2998, 2016.
- Bellouin, N., Rae, J., Jones, A., Johnson, C., Haywood, J., and Boucher, O.: Aerosol forcing in the Climate Model Intercomparison Project (CMIP5) simulations by HadGEM2-ES and the role of ammonium nitrate, *Journal of Geophysical Research: Atmospheres*, 116, D20206, 10.1029/2011JD016074, 2011.
- Bellouin, N., Baker, L., Hodnebrog, Ø., Olivié, D., Cherian, R., Macintosh, C., Samset, B., Esteve, A., Aamaas, B., Quaas, J., and Myhre, G.: Regional and seasonal radiative forcing by perturbations to aerosol and ozone precursor emissions, *Atmospheric Chemistry and Physics Discussion*, 10.5194/acp-2016-310, 2016.
- Bentsen, M., Bethke, I., Debernard, J. B., Iversen, T., Kirkevåg, A., Seland, Ø., Drange, H., Roelandt, C., Seierstad, I. A., Hoose, C., and Kristjánsson, J. E.: The Norwegian Earth System Model, NorESM1-M – Part 1: Description and basic evaluation of the physical climate, *Geosci. Model Dev.*, 6, 687-720, 10.5194/gmd-6-687-2013, 2013.
- Berntsen, T., Fuglestad, J. S., Joshi, M., Shine, K., Stuber, N., Li, L., Hauglustaine, D., and Ponater, M.: Climate response to regional emissions of ozone precursors: sensitivities and warming potentials, *Tellus B*, 57, 283-304, 2005.
- Berntsen, T., Fuglestad, J. S., Myhre, G., Stordal, F., and Berglen, T. F.: Abatement of greenhouse gases: Does location matter?, *Climatic Change*, 74, 377-411, 2006.
- Boer, G. B., and Yu, B. Y.: Climate sensitivity and response, *Climate Dynamics*, 20, 415-429, 10.1007/s00382-002-0283-3, 2003.
- Bond, T. C., Zarzycki, C., Flanner, M. G., and Koch, D. M.: Quantifying immediate radiative forcing by black carbon and organic matter with the Specific Forcing Pulse, *Atmos. Chem. Phys.*, 11, 1505-1525, 10.5194/acp-11-1505-2011, 2011.
- Bond, T. C., Doherty, S. J., Fahey, D. W., Forster, P. M., Berntsen, T., DeAngelo, B. J., Flanner, M. G., Ghan, S., Kärcher, B., Koch, D., Kinne, S., Kondo, Y., Quinn, P. K., Sarofim, M. C., Schultz, M. G., Schulz, M., Venkataraman, C., Zhang, H., Zhang, S., Bellouin, N., Guttikunda, S. K., Hopke, P. K., Jacobson, M. Z., Kaiser, J. W., Klimont, Z., Lohmann, U., Schwarz, J. P., Shindell, D., Storelvmo, T., Warren, S. G., and Zender, C. S.: Bounding the role of black carbon in the climate system: A scientific assessment, *Journal of Geophysical Research: Atmospheres*, 118, 5380–5552, 10.1002/jgrd.50171, 2013.
- Boucher, O., and Reddy, M. S.: Climate trade-off between black carbon and carbon dioxide emissions, *Energy Policy*, 36, 193-200, 2008.
- Bowerman, N. H. A., Frame, D. J., Huntingford, C., Lowe, J. A., Smith, S. M., and Allen, M. R.: The role of short-lived climate pollutants in meeting temperature goals, *Nature Clim. Change*, 3, 1021-1024, 10.1038/nclimate2034, 2013.

644 Bridgeman, C. H., Pyle, J. A., and Shallcross, D. E.: A three-dimensional model calculation of the ozone
645 depletion potential of 1-bromopropane (1-C₃H₇Br), *Journal of Geophysical Research: Atmospheres*,
646 105, 26493-26502, 10.1029/2000JD900293, 2000.

647 Collins, W. J., Sitch, S., and Boucher, O.: How vegetation impacts affect climate metrics for ozone
648 precursors, *J. Geophys. Res.*, 115, D23308, 10.1029/2010jd014187, 2010.

649 Collins, W. J., Fry, M. M., Yu, H., Fuglestad, J. S., Shindell, D. T., and West, J. J.: Global and regional
650 temperature-change potentials for near-term climate forcers, *Atmos. Chem. Phys.*, 13, 2471-2485,
651 10.5194/acp-13-2471-2013, 2013.

652 Daniel, J., Solomon, S., Sanford, T., McFarland, M., Fuglestad, J., and Friedlingstein, P.: Limitations
653 of single-basket trading: lessons from the Montreal Protocol for climate policy, *Climatic Change*, 111,
654 241-248, 10.1007/s10584-011-0136-3, 2012.

655 Fry, M. M., Naik, V., West, J. J., Schwarzkopf, D., Fiore, A., Collins, W. J., Dentener, F., Shindell, D. T.,
656 Atherton, C. S., Bergmann, D. J., Duncan, B. N., Hess, P. G., MacKenzie, I. A., Marmer, E., Schultz, M.
657 G., Szopa, S., Wild, O., and Zeng, G.: The influence of ozone precursor emissions from four world
658 regions on tropospheric composition and radiative climate forcing, *J. Geophys. Res.*, 117, D07306,
659 10.1029/2011JD017134, 2012.

660 Fuglestad, J. S., Berntsen, T. K., Isaksen, I. S. A., Mao, H., Liang, X.-Z., and Wang, W.-C.: Climatic
661 forcing of nitrogen oxides through changes in tropospheric ozone and methane; global 3D model
662 studies, *Atmospheric Environment*, 33, 961-977, 10.1016/s1352-2310(98)00217-9, 1999.

663 Fuglestad, J. S., Berntsen, T., Godal, O., and Skovdin, T.: Climate implications of GWP-based
664 reductions in greenhouse gas emissions, *Geophysical Research Letters*, 27, 409-412, 2000.

665 Fuglestad, J. S., Berntsen, T. K., Godal, O., Sausen, R., Shine, K. P., and Skovdin, T.: Metrics of
666 climate change: Assessing radiative forcing and emission indices, *Climatic Change*, 58, 267-331, 2003.

667 Fuglestad, J. S., Shine, K. P., Berntsen, T., Cook, J., Lee, D. S., Stenke, A., Skeie, R. B., Velders, G. J. M.,
668 and Waitz, I. A.: Transport impacts on atmosphere and climate: Metrics, *Atmospheric Environment*,
669 44, 4648-4677, 2010.

670 Hewitt, H. T., Copsey, D., Culverwell, I. D., Harris, C. M., Hill, R. S. R., Keen, A. B., McLaren, A. J., and
671 Hunke, E. C.: Design and implementation of the infrastructure of HadGEM3: the next-generation Met
672 Office climate modelling system, *Geosci. Model Dev.*, 4, 223-253, 10.5194/gmd-4-223-2011, 2011.

673 Hodnebrog, Ø., Myhre, G., and Samset, B. H.: How shorter black carbon lifetime alters its climate
674 effect, *Nat Commun*, 5, 10.1038/ncomms6065, 2014.

675 Holmes, C. D., Tang, Q., and Prather, M. J.: Uncertainties in climate assessment for the case of
676 aviation NO, *Proceedings of the National Academy of Sciences*, 10.1073/pnas.1101458108, 2011.

677 IPCC: *Climate Change: The IPCC Scientific Assessment*, edited by: Houghton, J. T., Jenkins, G. J., and
678 Ephraums, J. J., Cambridge University Press, Cambridge, United Kingdom, 1990.

679 IPCC: *The Physical Science Basis. Contribution of Working Group I to the Fifth Assessment Report of*
680 *the Intergovernmental Panel on Climate Change*, edited by: Stocker, T. F., Qin, D., Plattner, G. K.,
681 Tignor, M., Allen, S. K., Boschung, J., Nauels, A., Xia, Y., Bex, V., and Midgley, P. M., Cambridge
682 University Press, Cambridge, United Kingdom and New York, NY, USA, 1535 pp., 2013.

683 Iversen, T., Bentsen, M., Bethke, I., Debernard, J. B., Kirkevåg, A., Seland, Ø., Drange, H., Kristjansson,
684 J. E., Medhaug, I., Sand, M., and Seierstad, I. A.: The Norwegian Earth System Model, NorESM1-M –
685 Part 2: Climate response and scenario projections, *Geosci. Model Dev.*, 6, 389-415, 10.5194/gmd-6-
686 389-2013, 2013.

687 Jackson, S. C.: Parallel Pursuit of Near-Term and Long-Term Climate Mitigation, *Science*, 326, 526-527,
688 10.1126/science.1177042, 2009.

689 Joos, F., Roth, R., Fuglestad, F. S., Peters, G., Enting, I., Brovkin, V., Eby, M., Edwards, N. R., Burke, E.
690 J., Friedrich, T., Frölicher, T. L., Halloran, P., Holden, P. B., Jones, C., Kleinen, T., Mackenzie, F.,
691 Matsumoto, K., Meinshausen, M., Plattner, G.-K., Reisinger, A., Ridgwell, A., Shaffer, G., Segschneider,
692 J., Steinacher, M., Strassmann, K., Tanaka, K., Timmermann, A., Von Bloh, W., and Weaver, A.: Carbon
693 dioxide and climate impulse response functions for the computation of greenhouse gas metrics: A
694 multi-model analysis, *Atmospheric Chemistry and Physics*, 13, 2793-2825, 2013.

Klimont, Z., Höglund, L., Heyes, C., Purohit, P., Cofala, J., Borken-Kleefeld, J., Purohit, P., Kupiainen, K.,
 Winiwarter, W., Amann, M., Zhao, B., Wang, S. X., Bertok, I., and Sander, R.: Global scenarios of air
 pollutants and methane: 1990-2050, In prep.
 Lund, M., Berntsen, T., Fuglestad, J., Ponater, M., and Shine, K.: How much information is lost by
 using global-mean climate metrics? an example using the transport sector, *Climatic Change*, 113,
 949-963, 10.1007/s10584-011-0391-3, 2012.
 Intended Nationally Determined Contribution:
<http://www4.unfccc.int/submissions/INDC/Published%20Documents/Mexico/1/MEXICO%20INDC%2003.30.2015.pdf>,
 access: 06.30.2015, 2015.
 Myhre, G., Berglen, T. F., Johnsrud, M., Hoyle, C. R., Berntsen, T. K., Christopher, S. A., Fahey, D. W.,
 Isaksen, I. S. A., Jones, T. A., Kahn, R. A., Loeb, N., Quinn, P., Remer, L., Schwarz, J. P., and Yttri, K. E.:
 Modelled radiative forcing of the direct aerosol effect with multi-observation evaluation, *Atmos.*
Chem. Phys., 9, 1365-1392, 10.5194/acp-9-1365-2009, 2009.
 Myhre, G., Fuglestad, J. S., Berntsen, T. K., and Lund, M. T.: Mitigation of short-lived heating
 components may lead to unwanted long-term consequences, *Atmospheric Environment*, 45, 6103-
 6106, <http://dx.doi.org/10.1016/j.atmosenv.2011.08.009>, 2011.
 Myhre, G., Shindell, D., Bréon, F.-M., Collins, B., Fuglestad, J. S., Huang, J., Koch, D., Lamarque, J.-F.,
 Lee, D., Mendoza, B., Nakajima, T., Robock, A., Stephens, G., Takemura, T., and Zhang, H.:
 Anthropogenic and Natural Radiative Forcing, in: *Climate Change 2013: The Physical Science Basis.*
 Contribution of Working Group I to the Fifth Assessment Report of the Intergovernmental Panel on
 Climate Change, edited by: Stocker, T. F., Qin, D., Plattner, G. K., Tignor, M., Allen, S. K., Boschung, J.,
 Nauels, A., Xia, Y., Bex, V., and Midgley, P. M., Cambridge University Press, Cambridge, United
 Kingdom and New York, NY, USA, 2013.
 Naik, V., Mauzerall, D., Horowitz, L., Schwarzkopf, M. D., Ramaswamy, V., and Oppenheimer, M.: Net
 radiative forcing due to changes in regional emissions of tropospheric ozone precursors, *J. Geophys.*
Res., 110, D24306, 10.1029/2005jd005908, 2005.
 Olivé, D. J. L., and Peters, G.: Variation in emission metrics due to variation in CO₂ and temperature
 impulse response functions, *Earth System Dynamics*, 4, 267-286, 10.5194/esd-4-267-2013, 2013.
 Olsen, S. C., Hannegan, B. J., Zhu, X., and Prather, M. J.: Evaluating ozone depletion from very short-
 lived halocarbons, *Geophysical Research Letters*, 27, 1475-1478, 10.1029/1999GL011040, 2000.
 Paoli, R., Cariolle, D., and Sausen, R.: Review of effective emissions modeling and computation,
Geosci. Model Dev., 4, 643-667, 10.5194/gmd-4-643-2011, 2011.
 Peters, G., Aamaas, B., Berntsen, T., and Fuglestad, F. S.: The integrated Global Temperature
 Change Potential (iGTP) and relationship with other simple emission metrics, *Environmental*
Research Letters, 6, 044021, 10.1088/1748-9326/6/4/044021, 2011.
 Pierrehumbert, R.: Short-Lived Climate Pollution, *Annual Review of Earth and Planetary Sciences*, 42,
 341-379, 10.1146/annurev-earth-060313-054843, 2014.
 Prather, M. J.: Lifetimes of atmospheric species: Integrating environmental impacts, *Geophysical*
Research Letters, 29, 20-21-20-23, 10.1029/2002GL016299, 2002.
 Rogelj, J., Schaeffer, M., Meinshausen, M., Shindell, D. T., Hare, W., Klimont, Z., Velders, G. J. M.,
 Amann, M., and Schellnhuber, H. J.: Disentangling the effects of CO₂ and short-lived climate forcer
 mitigation, *Proceedings of the National Academy of Sciences*, 111, 16325-16330,
 10.1073/pnas.1415631111, 2014.
 Rypdal, K., Berntsen, T., Fuglestad, J. S., Aunan, K., Torvanger, A., Stordal, F., Pacyna, J. M., and
 Nygaard, L. P.: Tropospheric ozone and aerosols in climate agreements: scientific and political
 challenges, *Environmental Science and Policy*, 8, 29-43, 10.1016/j.envsci.2004.09.003, 2005.
 Sarofim, M.: The GTP of Methane: Modeling Analysis of Temperature Impacts of Methane and
 Carbon Dioxide Reductions, *Environmental Modeling and Assessment*, 17, 231-239, 10.1007/s10666-
 011-9287-x, 2012.
 Schmale, J., Shindell, D., von Schneidmesser, E., Chabay, I., and Lawrence, M.: Clean up our skies,
Nature, 515, 335-337, 2014.

746 Shindell, D., and Faluvegi, G.: Climate response to regional radiative forcing during the twentieth
 747 century, *Nature Geoscience*, 2, 294-300, 2009.
 748 Shindell, D., Schulz, M., Ming, Y., Takemura, T., Faluvegi, G., and Ramaswamy, V.: Spatial scales of
 749 climate response to inhomogeneous radiative forcing, *Journal of Geophysical Research: Atmospheres*,
 750 115, D19110, 10.1029/2010JD014108, 2010.
 751 Shindell, D. T., Faluvegi, G., Koch, D. M., Schmidt, G. A., Unger, N., and Bauer, S. E.: Improved
 752 Attribution of Climate Forcing to Emissions, *Science*, 326, 716-718, 10.1126/science.1174760, 2009.
 753 Shine, K. P., Fuglestad, J. S., Hailemariam, K., and Stuber, N.: Alternatives to the Global Warming
 754 Potential for Comparing Climate Impacts of Emissions of Greenhouse Gases, *Climatic Change*, 68,
 755 281-302, 10.1007/s10584-005-1146-9, 2005.
 756 Shine, K. P., Berntsen, T., Fuglestad, J. S., Stuber, N., and Skeie, R. B.: Comparing the climate effect
 757 of emissions of short and long lived climate agents, *Philosophical Transactions of the Royal Society A*,
 758 365, 1903-1914, 2007.
 759 Shoemaker, J. K., Schrag, D. P., Molina, M. J., and Ramanathan, V.: What Role for Short-Lived Climate
 760 Pollutants in Mitigation Policy?, *Science*, 342, 1323-1324, 10.1126/science.1240162, 2013.
 761 Smith, S. J., and Mizrahi, A.: Near-term climate mitigation by short-lived forcers, *Proceedings of the*
 762 *National Academy of Sciences*, 110, 14202-14206, 10.1073/pnas.1308470110, 2013.
 763 Solomon, S., Daniel, J. S., Sanford, T. J., Murphy, D. M., Plattner, G.-K., Knutti, R., and Friedlingstein, P.:
 764 Persistence of climate changes due to a range of greenhouse gases, *Proceedings of the National*
 765 *Academy of Sciences*, 107, 18354-18359, 10.1073/pnas.1006282107, 2010.
 766 Stevens, B., Giorgetta, M., Esch, M., Mauritsen, T., Crueger, T., Rast, S., Salzmann, M., Schmidt, H.,
 767 Bader, J., Block, K., Brokopf, R., Fast, I., Kinne, S., Kornblueh, L., Lohmann, U., Pincus, R., Reichler, T.,
 768 and Roeckner, E.: Atmospheric component of the MPI-M Earth System Model: ECHAM6, *Journal of*
 769 *Advances in Modeling Earth Systems*, 5, 146-172, 10.1002/jame.20015, 2013.
 770 Streets, D. G., Bond, T. C., Carmichael, G. R., Fernandes, S. D., Fu, Q., He, D., Klimont, Z., Nelson, S. M.,
 771 Tsai, N. Y., Wang, M. Q., Woo, J. H., and Yarber, K. F.: An inventory of gaseous and primary aerosol
 772 emissions in Asia in the year 2000, *Journal of Geophysical Research: Atmospheres*, 108, 8809,
 773 10.1029/2002JD003093, 2003.
 774 Sørve, O. A., Gauss, M., Smyshlyaev, S. P., and Isaksen, I. S. A.: Evaluation of the chemical transport
 775 model Oslo CTM2 with focus on arctic winter ozone depletion, *Journal of Geophysical Research:*
 776 *Atmospheres*, 113, n/a-n/a, 10.1029/2007JD009240, 2008.
 777 Tanaka, K., Peters, G. P., and Fuglestad, J. S.: Multi-component climate policy: why do emission
 778 metrics matter?, *Carbon Management*, 1, 191-197, 2010.
 779 Tol, R. S. J., Berntsen, T., O'Neill, B. C., Fuglestad, J. S., and Shine, K.: A unifying framework for
 780 metrics for aggregating the climate effect of different emissions *Environmental Research Letters*, 7,
 781 044006, 10.1088/1748-9326/7/4/044006, 2012.
 782 Victor, D., and Kennel, C. F.: Ditch the 2°C warming goal, *Nature*, 514, 30-31, 10.1038/514030a 2014.
 783 Wild, O., Prather, M. J., and Akimoto, H.: Indirect long-term global radiative cooling from NO_x
 784 emissions, *Geophys. Res. Lett.*, 28, 1719-1722, 10.1029/2000gl012573, 2001.
 785 Wuebbles, D. J., Patten, K. O., Johnson, M. T., and Kotamarthi, R.: New methodology for Ozone
 786 Depletion Potentials of short-lived compounds: n-Propyl bromide as an example, *Journal of*
 787 *Geophysical Research: Atmospheres*, 106, 14551-14571, 10.1029/2001JD900008, 2001.
 788 Yu, H., Chin, M., West, J. J., Atherton, C. S., Bellouin, N., Bergmann, D., Bey, I., Bian, H., Diehl, T.,
 789 Forberth, G., Hess, P., Schulz, M., Shindell, D., Takemura, T., and Tan, Q.: A multimodel assessment of
 790 the influence of regional anthropogenic emission reductions on aerosol direct radiative forcing and
 791 the role of intercontinental transport, *Journal of Geophysical Research: Atmospheres*, 118, 700-720,
 792 10.1029/2012JD018148, 2013.

793

794

795 Table 1: General circulation models (GCM) and chemistry transport models (CTM) used to calculate
 796 radiative forcing in this study. Resolution shows the horizontal resolution and the number of vertical
 797 layers. Radiative forcing has been calculated for emissions of these gases and particles by Bellouin et
 798 al. (2016).

Model	Type	Resolution	BC	OC	SO ₂	NH ₃	NO _x	CO	VOC	CH ₄	References
ECHAM6- HAMMOZ	GCM	1.8°x1.8° L31	X	X	X						Stevens et al. (2013)
HadGEM3- GLOMAP	GCM	1.8°x1.2° L38	X	X	X		X	X	X	X	Hewitt et al. (2011)
NorESM	GCM	1.9°x2.5° L26	X	X	X		X	X	X	X	Bentsen et al. (2013);Iversen et al. (2013)
OsloCTM2	CTM	2.8°x2.8° L60	X	X	X	X	X	X	X	X	Søvde et al. (2008);Myhre et al. (2009)

799

800

801

802 Table 2: The best estimate given for GTP(20) values. The component of each species which the mass
 803 emission refers to is shown in brackets. The regions are Europe (EUR), East Asia (EAS), shipping (SHP),
 804 and global (GLB), for emissions occurring in NH summer, May-October, (s) and NH winter, November-
 805 April, (w).

GTP(20)	BC [C]	OC [C]	SO ₂ [SO ₂]	NH ₃ [NH ₃]	NO _x [N]	CO [CO]	VOC [C]	CH ₄ [CH ₄]
	<u>620</u>							48
EUR, s	570	-220	-130	-16	-90	4.3	23	
	<u>530</u>							48
EUR, w	490	-110	-36-41	-10	-40	4.9	14	
	<u>610</u>							48
EAS, s	390	-140	-87-74	-7.7	-75	4.5	19	
	<u>330</u>							48
EAS, w	329	-50	-31-30	-15	-75	5.0	8.9	
	<u>390</u>							48
SHP, NH s	480	-620	-160	NA	-230	4.7	32	
	<u>470</u>							48
SHP, NH w	510	-310	-110	NA	-400	5.9	30	
								48
	<u>810</u>	260-						
GLB, NH s	600	200	-120	-7.2	-150	4.4	22	
								48
	<u>600</u>	190-						
GLB, NH w	570	160	-67-70	-11	-160	4.9	21	

806

807

Figure 1: Pulse, sustained, and ramping-up emission profiles. The ramping-up period can vary.

Figure 2: GTP(20) values for the species, for all regions and seasons, decomposed by processes. The regions included are Europe (EUR), East Asia (EAS), shipping (SHP), and global (GLB), all for both NH summer, May-October, (s) and NH winter, November-April, (w). How the best estimate of the net effect is calculated is given in Sect. 2.1. The uncertainty bars show the range across models, which is not given for shipping as the best estimate is based on only two models for that sector.

Figure 3: GWP(100) values for the ozone precursors, for all regions and seasons, decomposed by processes. The regions included are Europe (EUR), East Asia (EAS), shipping (SHP), and global (GLB), all for both NH summer, May-October, (s) and NH winter, November-April, (w). How the best estimate of the net effect is calculated is given in Sect. 2.1. The uncertainty bars show the range across models, which is not given for shipping as the best estimate is based on only two models for that sector.

Figure 4: Scatter plot of the normalized variability of the model estimates (NV_m) versus NVBE for the best estimate. Colors of the symbols indicate individual models (red: OsloCTM2, green: NorESM, blue: HadGEM3, and light blue: ECHAM6) and the shape of the symbol indicate individual species. Left panel: Aerosols and aerosol precursors (BC, OC, and SO_2). Right panel: Ozone precursors (NO_x , CO, and VOC). The black line is the one-to-one line. The estimates use the GTP(20) emission metric.

Figure 5: Emission metric-based estimate of change in global mean temperature by 10% reduction in emissions of all SLCFs based on 2008 global emissions with positive best estimate AGTP(20) values (BC, CO, and VOC, labelled B), and 10% global reduction of all SLCFs (also including OC, SO_2 , and NO_x , labelled A). Colored symbols use sets of emission metrics from individual models. The blue bar is given based on summing contributions using all MAXs and MINs in Fig. 2. The black bar is the uncertainty assuming the metric estimates are all independent.

Figure 6: A comparison of GTP values, as a function of time horizon, for summer emissions in Europe (left) and East Asia (right).

Figure 7: GTPs (top) and GWPs (bottom) for BC (left) and NO_x (right) as a function of time horizon, for all emission cases.

Figure 8: The global temperature response 10, 20, 50, and 100 years after regional and seasonal emissions in 2008. The regions from top to bottom are Europe, East Asia, the global shipping sector,

844 and global. NH summer season (May-October) is to the left, NH winter season (November-April) to
845 the right. Note that the y-axis differs between the regions.

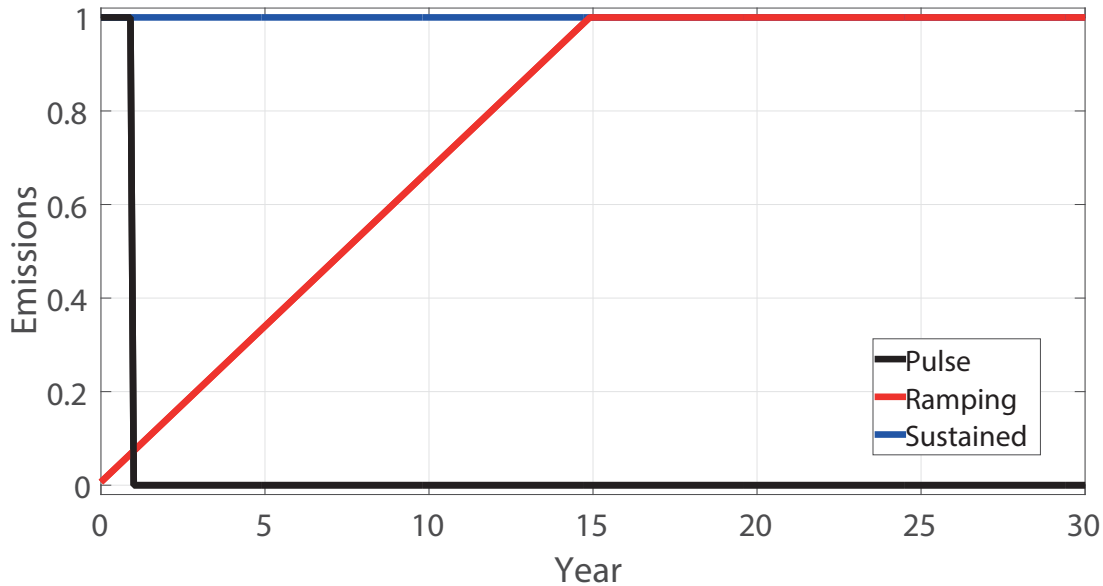
846

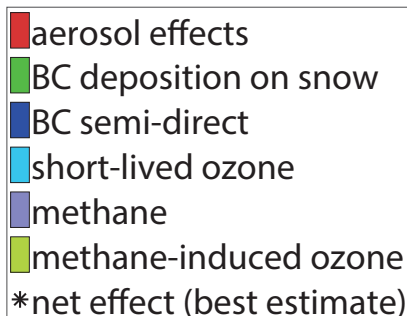
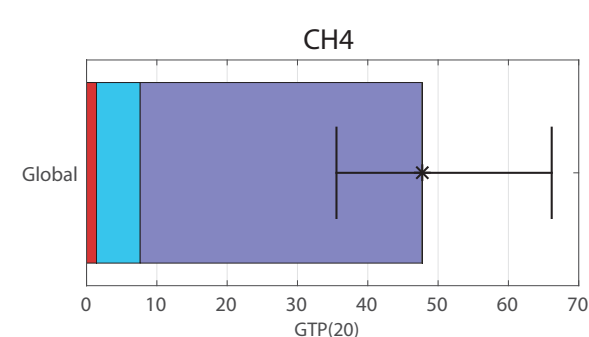
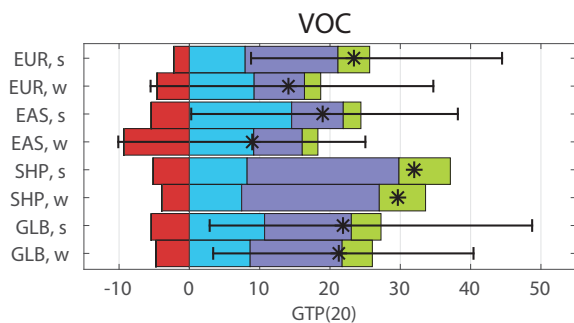
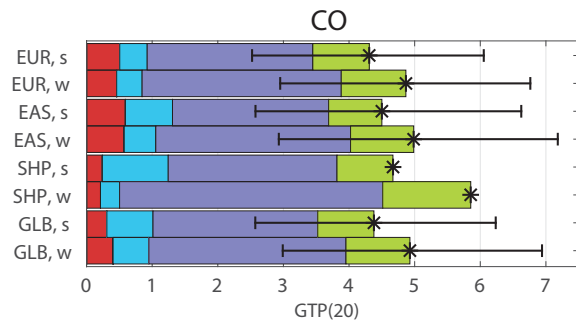
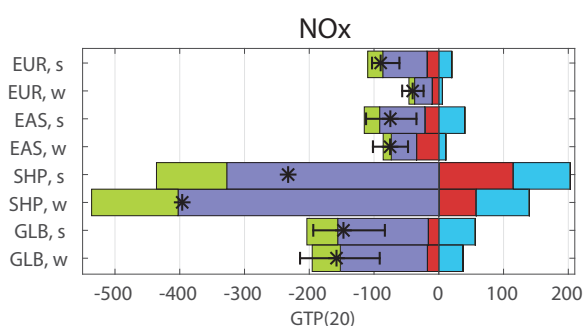
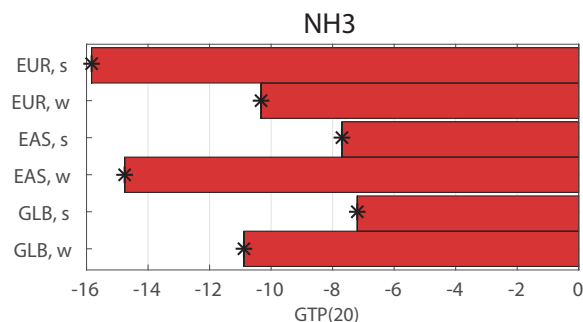
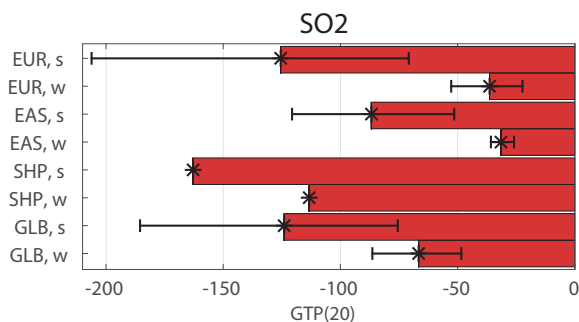
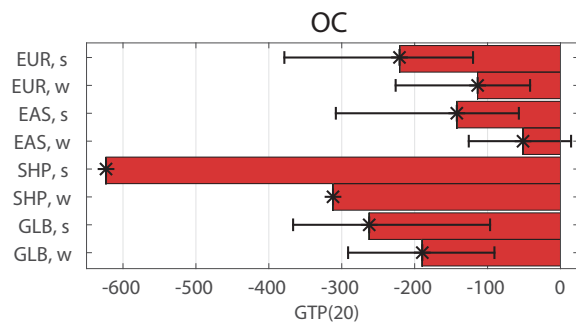
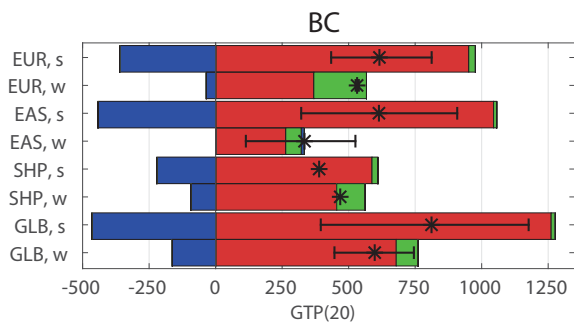
847 Figure 9: The emission metric values for different types of emission profiles for European emissions
848 in summer, GTP to the left and GWP to the right. The ramping-up period is set to 15 years. We
849 include NO_x, CO, and VOC (top) as ozone precursors that include processes that alter the
850 atmospheric chemistry both on monthly and yearly scales and BC (middle) representing particle
851 emissions with an atmospheric lifetime of about a week. To set in perspective, we also show for CH₄
852 (bottom), which perturbs the atmosphere with a lifetime of roughly 12 years.

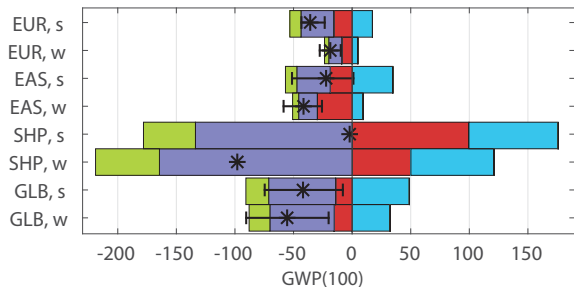
853

854 Figure 10: The emission metric values for ramping-up scenario emissions. GTP (top) and GWP
855 (bottom) are given for BC (left) and NO_x (right).

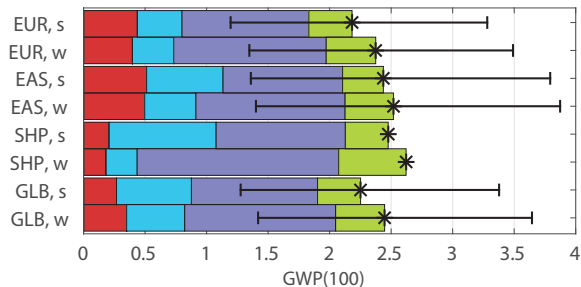
Emission profiles



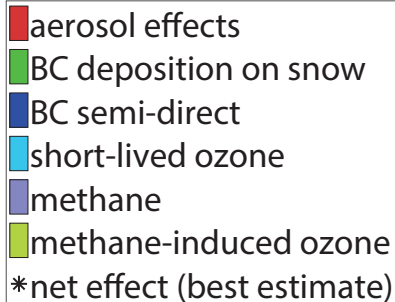
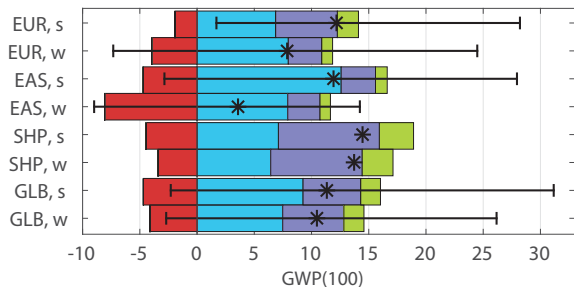


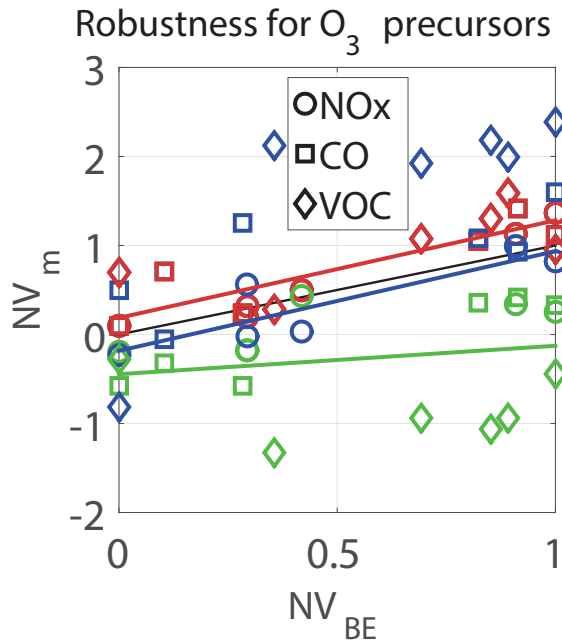
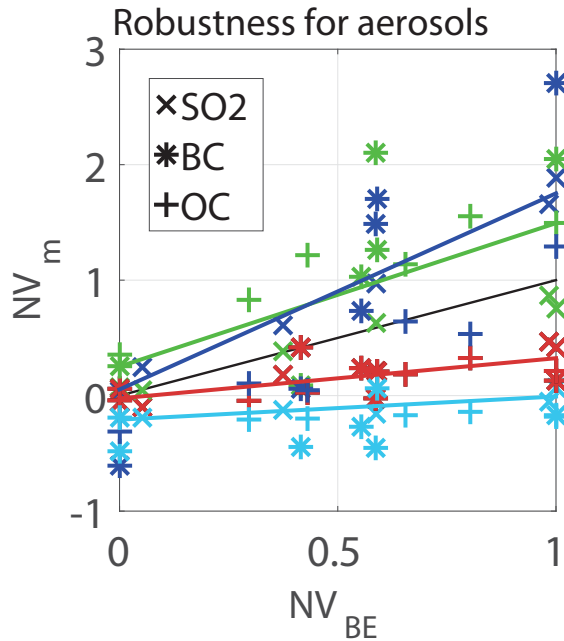
NO_x

CO

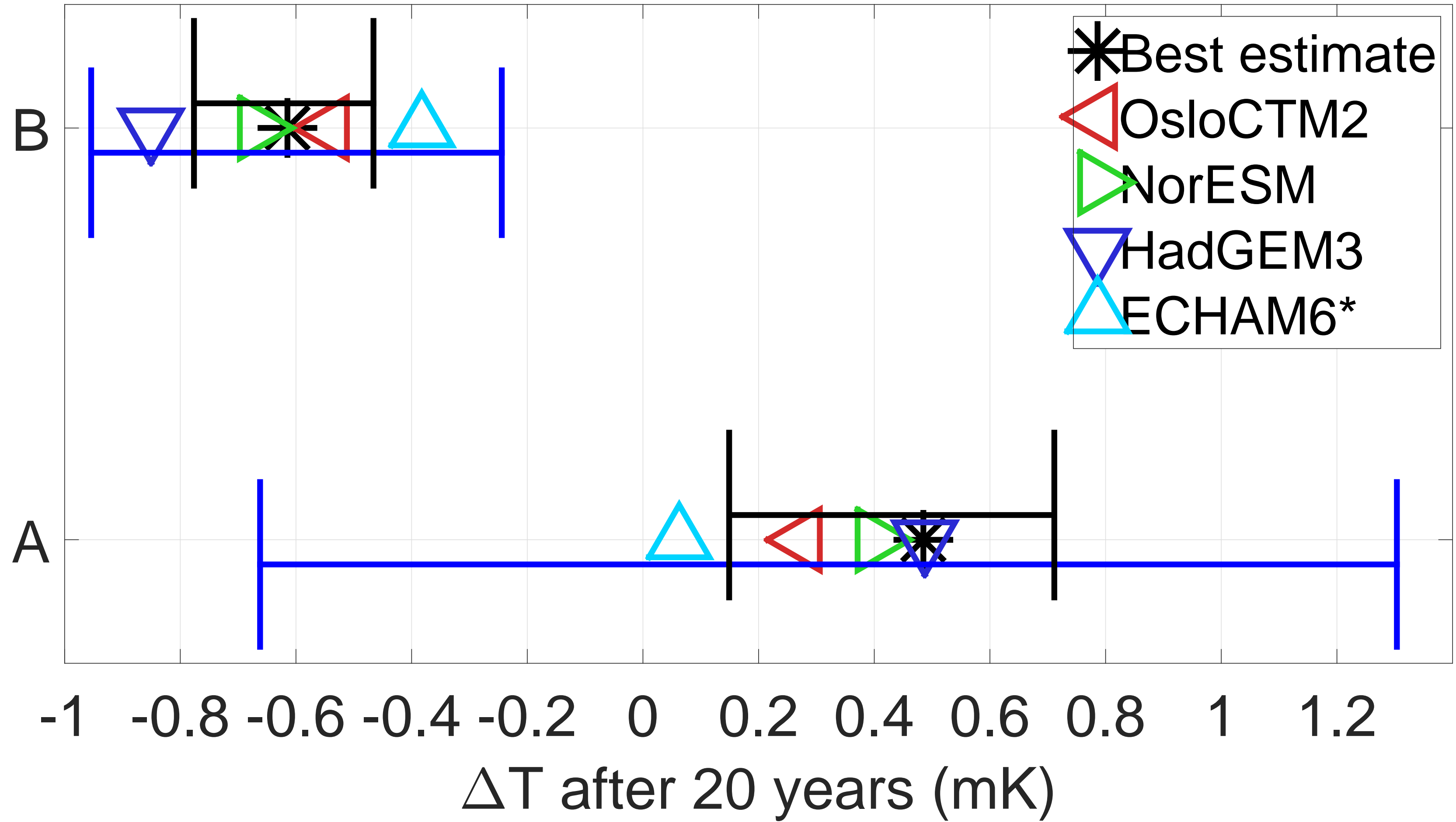


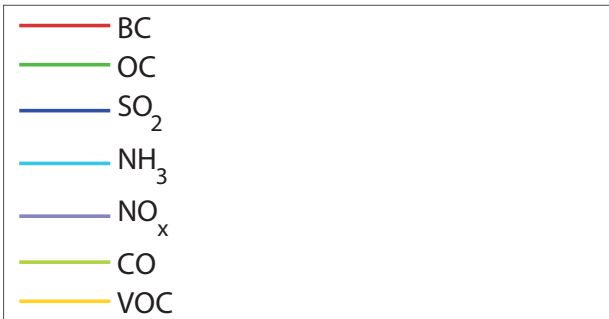
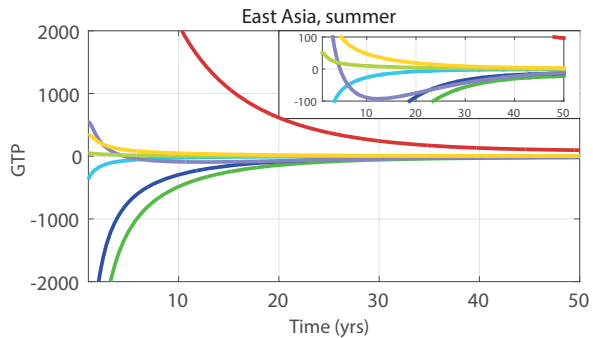
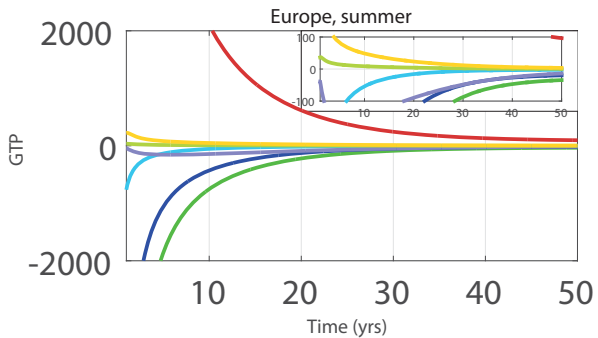
VOC

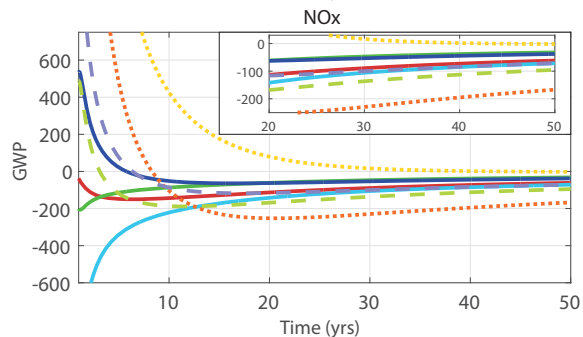
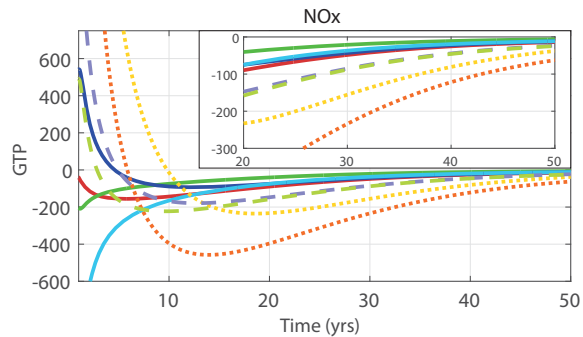
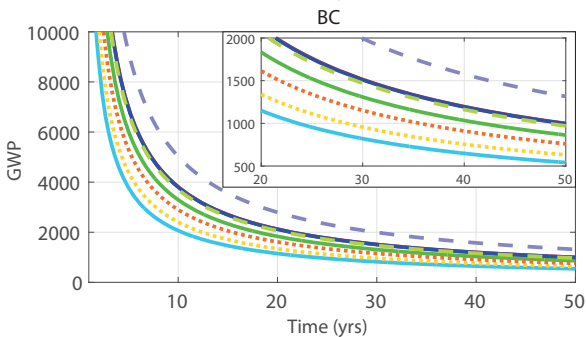
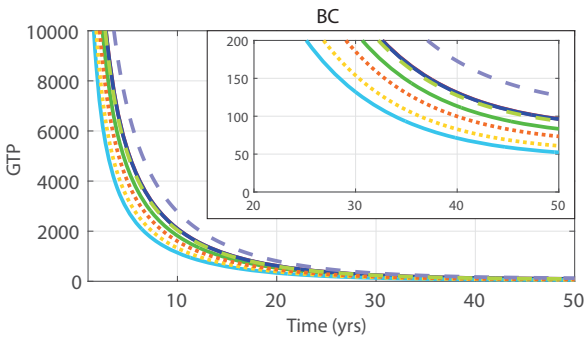




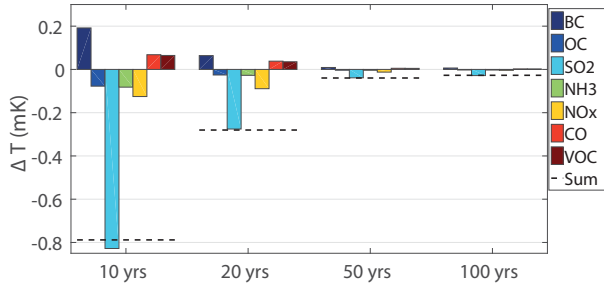
Robustness in total climate impact



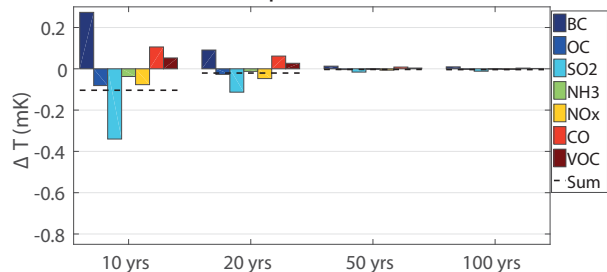




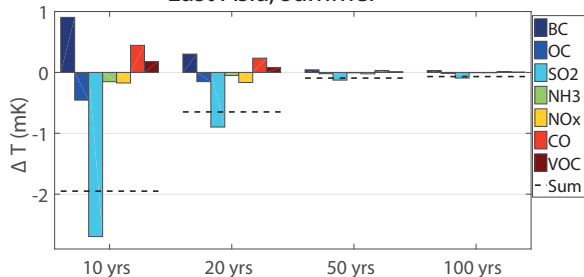
Europe, summer



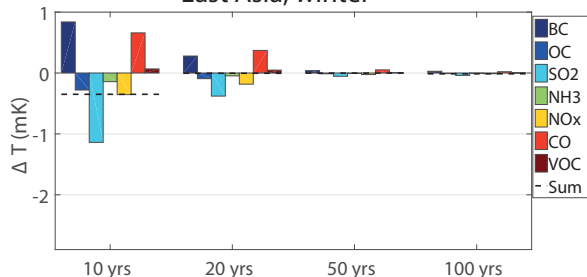
Europe, winter



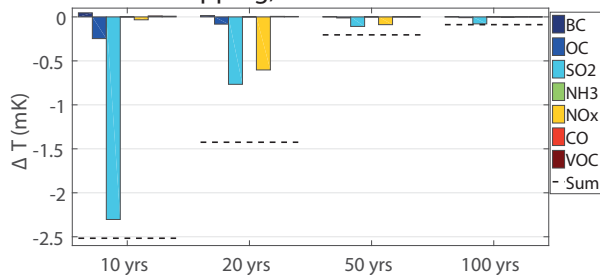
East Asia, summer



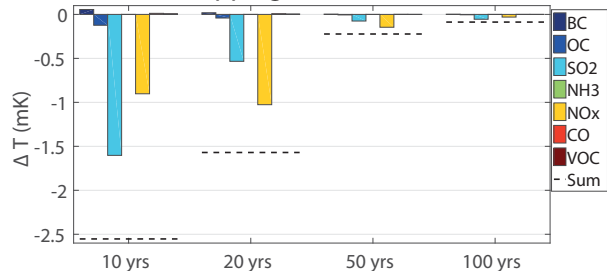
East Asia, winter



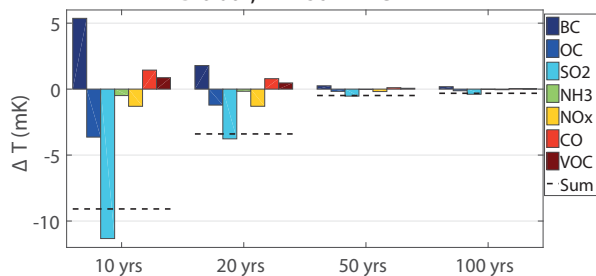
Shipping, NH summer



Shipping, NH winter



Global, NH summer



Global, NH winter

